Journal of Polymer Research (2023) 30:356
https://doi.org/10.1007/s10965-023-03712-8

ORIGINAL PAPER

Electroactive modified poly(2-aminobenzoic acid)-blend-aloe vera/GCE as an efficient dopamine sensor

Julia Sebastian[1] · Miriam Daniel[2] · Bernaurdshaw Neppolian[2] · Jhancy Mary Samuel[1]

Received: 16 February 2023 / Accepted: 24 July 2023 / Published online: 22 August 2023

Abstract

We report an electrochemical biosensor based on poly(2-aminobenzoic acid)-blend-aloe vera (PABA-AV) synthesized by emulsion polymerization and fabricated for sensing dopamine. The sensing behaviour of poly(2-aminobenzoic acid) was also investigated. The structure, morphology, thermal, electrical, and electrochemical properties were characterized by FTIR, UV-Visible, XRD, SEM-EDX, TGA and DTA, EIS, CV and DPV. The electrical conductivities of PABA and PABA/AV are 1.5 $x10^{-3}$ S cm^{-1} and 1.85 $x10^{-3}$ S cm^{-1} respectively. Modified PABA-AV/GCE oxidizes dopamine at a higher anodic current of 73.5 µA in comparison to bare GCE and PABA/GCE. Electroactive modified PABA-AV/GCE exhibited an excellent response to DA concentration in the wide linear range of 100-800 µM (R^2= 0.9982) with a detection limit of 0.0517 µM (S/N=3) and a limit of quantification of 0.1722 µM (S/N=10). It exhibited excellent sensitivity, selectivity, repeatability, reproducibility and stability towards dopamine suggesting it as a promising material for sensing dopamine.

Keywords Poly(2-aminobenzoic acid) · Aloe vera · Emulsion polymerization · Dopamine · Electrochemical biosensor

Introduction

Dopamine (DA) (3,4-Dihydroxyphenylethylamine) belongs to the class of naturally existing catecholamines and is vital for the well-being of the cardiovascular, renal, hormonal and central nervous systems. The malfunctioning or insufficiency of DA leads to neurological disorders such as Parkinson's disease, Schizophrenia, Huntington's disease etc. On the other hand, excessive DA secretion is associated with dysfunction in energy metabolism. This suggests that the detection and quantification of DA are essential in the prevention, diagnosis and treatment of the above disorders [1, 2]. Several analytical techniques have been employed for the detection of DA such as flow injection chemiluminescence, high-performance liquid chromatography, liquid chromatography-tandem mass spectrometry, capillary electrophoresis with laser-induced native fluorescence and electrochemical analysis [3–6]. Easy operation, affordability, high specificity and quick analysis are the added benefits of the electrochemical method [7]. The greatest challenge in the electrochemical detection of DA is the occurrence of co-existing interferences like ascorbic acid and uric acid in the body fluid, which have equivalent oxidation potentials as DA. Thus, several attempts have been made to modify electrodes for the detection including organic redox mediators, nanoparticles, polymers, self-assembled monolayers and carbon nanotubes [8–11].

Low dosage of DA causes severe symptoms of Parkinson's disease. The prolonged administration of Aloe vera (*Aloe barbadensis miller*) belonging to the family Liliaceae assists in the rise of DA level due to the analgesic property of aloe vera [12]. Plant-based carbon materials can also be efficient in the detection of dopamine. An eco-friendly synthesis of iron oxide (ɣ - Fe_2O_3) nanoparticles in various morphologies such as aggregates, nanobelts, and nanodots by aloe vera extract mediated by the sol-gel method have been reported. ɣ - Fe_2O_3 nanobelts proved to have reasonably good sensitivity and selectivity towards dopamine and uric acid in the linear range of 1.2 µM – 0.031 mM. The anodic peak current also increased successively with increased concentration of DA with a correlation factor of R^2 = 0.9970 [13].

✉ Jhancy Mary Samuel
jmarys@auxiliumcollege.edu.in; jhancy2011@gmail.com

[1] Department of Chemistry, Auxilium College, Thiruvalluvar University, Serkkadu, Vellore, Tamil Nadu 632 115, India

[2] Department of Chemistry, SRM Institute of Science and Technology, Kattankulathur, Chennai, Tamil Nadu 603203, India

Among the conducting polymers, polyaniline and its derivatives have received considerable attention owing to its cost-effectiveness, ease of fabrication, excellent environmental stability, rich oxidation-reduction chemistry and promising electrical conductivity [14, 15]. A biosensor based on poly(o-methoxyaniline)/Au nanocomposite was developed by Sangamithirai et al. to sense dopamine and folic acid simultaneously with a detection limit of 0.062 µM in the linear range 10 to 300 µM for dopamine and a detection limit of 0.090 µM in the linear range 0.5 to 900 µM for folic acid [16]. The charge transport properties, redox behaviour and biocompatibility of poly(2-aminobenzoic acid) with π-conjugated backbones facilitate the transmission of the electrochemical signals to the electrode thereby increasing the electrocatalytic activity. The rich electron flow in poly(2-aminobenzoic acid) and the high electron density on the carboxyl groups facilitate the interaction between DA and poly(2-aminobenzoic acid) [17]. Gupta et al. fabricated poly(anthranilic acid)/Au nanocomposites dopamine sensor with a sensitivity of 12.5 µA ± 250 nA/mM and a detection limit of 1 µM. There was no interference of ascorbic acid on the developed sensor due to the presence of a carboxylic acid group on poly(anthranilic acid) [18]. CA 125 could be detected using poly(anthranilic acid) coated with gold and silver nanoparticles with acceptable stability, selectivity, sensitivity and repeatability of the immunosensors [19].

Thus, in this paper, we report the dopamine sensing capability of emulsion-polymerized poly(2-aminobenzoic acid)-blend-aloe vera that exhibited excellent conductivity and biocompatibility. The fabricated electrochemical biosensor proved outstanding sensitivity, selectivity, repeatability, reproducibility and stability towards dopamine extending its potential application in the field of biosensors.

Experimental section

Materials used

2-aminobenzoic acid was purchased from Avra Synthesis Pvt. Ltd., Camphor sulphonic acid (CSA) from Spectrochem Pvt. Ltd., India, Ammonium persulphate (APS) from Spectrum Reagents and Chemicals Pvt. Ltd., Kerala, India and Chloroform from Isochem Laboratories, Kerala, India The chemicals used for the electrochemical sensing studies were of analytical grade. *Aloe barbadensis miller* (AV) was selected as the plant-based material and authenticated by the Department of Botany, Auxilium College, Vellore-6.

Characterization

The materials were characterized by UV-Visible (UV-Vis) spectroscopy (Jasco V-670, Japan), Fourier Transform Infrared (FT-IR) spectroscopy (Nicolet iS50, Thermo Scientific, USA), Powder X-Ray Diffractometer (D8 Advance, Bruker, Germany) and Scanning Electron Microscopy (Tescan VEGA 3SBH with Bruker easy EDS, Czech Republic). Thermogravimetric analysis (TGA) (SDT Q600 TA Instruments, USA) and Differential Thermal Analysis (DTA) (SDT Q600 TA Instruments, USA) were performed at an inert N_2 atmosphere from room temperature to 800 °C at a heating rate of 20 °C/minute and the sample pans used were alumina. The electrical conductivity was measured using Model 660E Electrochemical analyzer, Shanghai, China. The sensing studies were performed electrochemically by an SP-150 BioLogic workstation.

Emulsion polymerization of PABA and PABA-AV

The monomer: oxidant ratio was 1:1 for the synthesis of PABA and 1:2 for PABA-AV. 50 ml $CHCl_3$ and 50 ml 0.1 M CSA were mixed and magnetically stirred to obtain a milky white emulsion, followed by the addition of 0.1 mol of 2-aminobenzoic acid. 100 ml 1 M HCl and 100 ml 0.1 mol APS were added dropwise and stirred continuously for 24 hours at 1000 rpm and allowed to settle to separate the aqueous and organic phases. The sedimented organic phase was filtered, washed repeatedly with deionized water and finally with methanol to eliminate the impurities and oligomers, dried and desiccated [20]. The same procedure was adopted to synthesize PABA-AV by adding 1.4 g (20 wt%) of aloe vera powder initially to the monomer respectively. PABA and PABA-AV appeared as brown powder with a percentage yield of 26.08 % and 57.97 % respectively.

Preparation of aloe vera powder

Fresh and healthy leaves of aloe vera were cut and left at room temperature to drain the toxic yellow liquid, Aloin, washed repeatedly with deionized water and methanol to remove the mud and impurities present on the outer rind. The thorn-like spikes were cut and the leaves were finely chopped, dried, finely powdered, sieved and stored at room temperature for further use.

Preparation of PABA-AV/GCE modified electrode

The modified PABA-AV/GCE was fabricated by dissolving 3 mg of finely powdered PABA-AV in 2 ml ethanol. 10 µl Nafion binder was added and ultrasonicated for half an hour to attain a uniform dispersion. 6 µl of the electrocatalyst was pipetted, drop cast onto the glassy carbon electrode and air dried for 15 minutes. The electrochemical analysis was performed in a three-electrode cell consisting of Ag/AgCl as a reference, Pt wire as a counter and GCE as the working electrode. The cyclic voltammetry was run at a scan rate of

50 mVs^{-1} using 0.1 M PBS maintained at pH=7 with 1mM DA unless specified otherwise.

Results and discussion

Characterization

The FTIR spectra of PABA and PABA-AV are presented in Fig. 1(a) and 1(b) respectively. In Fig. 1(a), a broad peak from 3700 to 2800 cm^{-1} (O-H stretching), 3182 cm^{-1} (N-H stretching), 1681 cm^{-1} (C=O stretching), 1583 cm^{-1} (quinonoid), 1510 cm^{-1} (benzenoid), 1041 cm^{-1} (symmetric, asymmetric stretching modes of SO_3^- of CSA), 1230 cm^{-1} (C-N stretching) 1170 cm^{-1} (electrical conductivity) [21], 943 cm^{-1} and 840 cm^{-1} (C-H out-of-plane bending vibration of 1,2,4-trisubstituted aromatic rings) confirm the polymerization. In PABA/AV, in addition to the characteristic peaks of PABA, it shows a peak at 1042 cm^{-1} corresponding to the mannopyranose present in aloe vera [22]. The interaction of aloe vera and poly(2-aminobenzoic acid) is based on hydrogen bonding as shown by the broadening of the OH stretching vibration.

Figure 2(a) and (b) represent the UV-Visible spectra of PABA and PABA-AV. PABA exhibits three absorptions centered at 245, 297 and 352 nm which are ascribed to π-π*, n-π* and polaronic transition state respectively and PABA/AV exhibits three absorptions at 222 nm, 293 nm and 393 nm. The hypsochromic shift indicates an increase in delocalization energy [23].

Figure 3(a) and (b) depict the XRD patterns of PABA and PABA-AV. The diffraction peaks are observed at 2θ = 16.7° and 25.7° in PABA and 2θ = 16.7°, 18.9° and 24.4° in PABA-AV. The XRD clearly depicts the semi-crystalline nature [24].

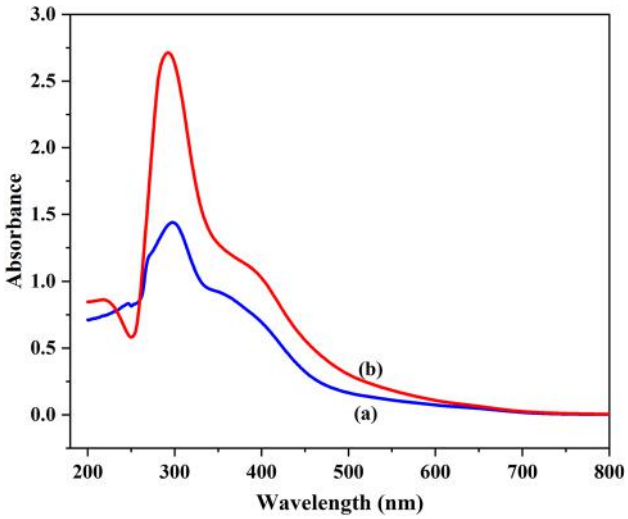

Fig. 2 UV-Visible spectra of (**a**) PABA (**b**) PABA-AV

The thermograms of PABA and PABA-AV are given in Fig. 4(a) and (b) respectively. The degradation occurs in three steps, water molecules are lost at 100 °C, dopant molecules between 150-400 °C and the decomposition of the polymer backbone starts at 400 °C [25, 26].

The exothermic breakdown of the polymeric components and the endothermic degradation of water molecules of PABA and PABA/AV are depicted in Fig.5(a) and (b) [27].

The SEM-EDX analysis of PABA-AV at a magnification of 10,000x is displayed in Fig. 6(a) and (b). The SEM image indicates an agglomerated and porous morphology. The elemental analysis shows the presence of inorganic elements such as Na, Mg, Ca, Cl, S, Fe in aloe vera in addition to C, N and O as represented in Table 1. The EDX of PABA/AV is a strong evidence for the incorporation of aloe vera in PABA.

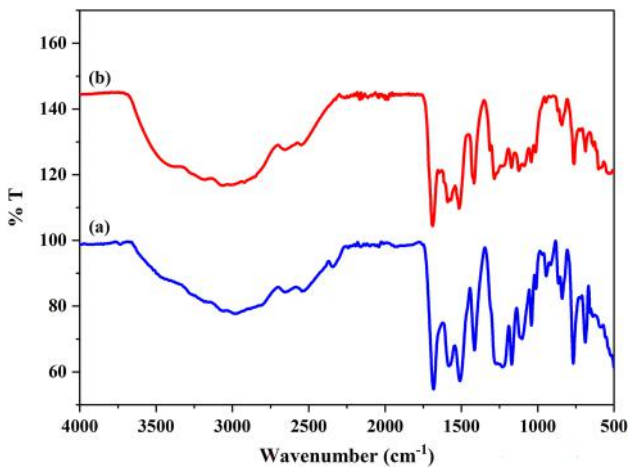

Fig. 1 FTIR spectra of (**a**) PABA (**b**) PABA-AV

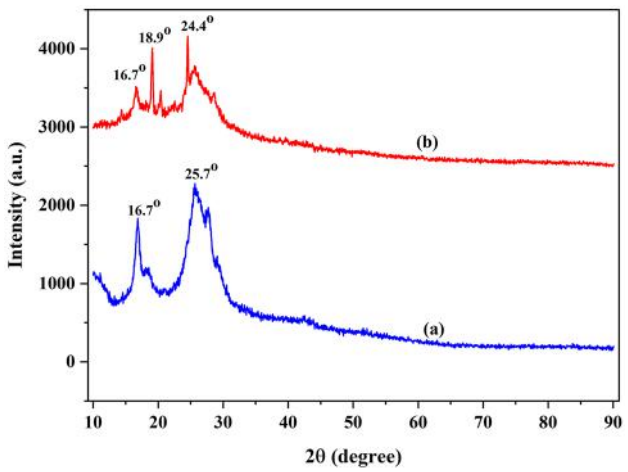

Fig. 3 XRD of (**a**) PABA (**b**) PABA-AV

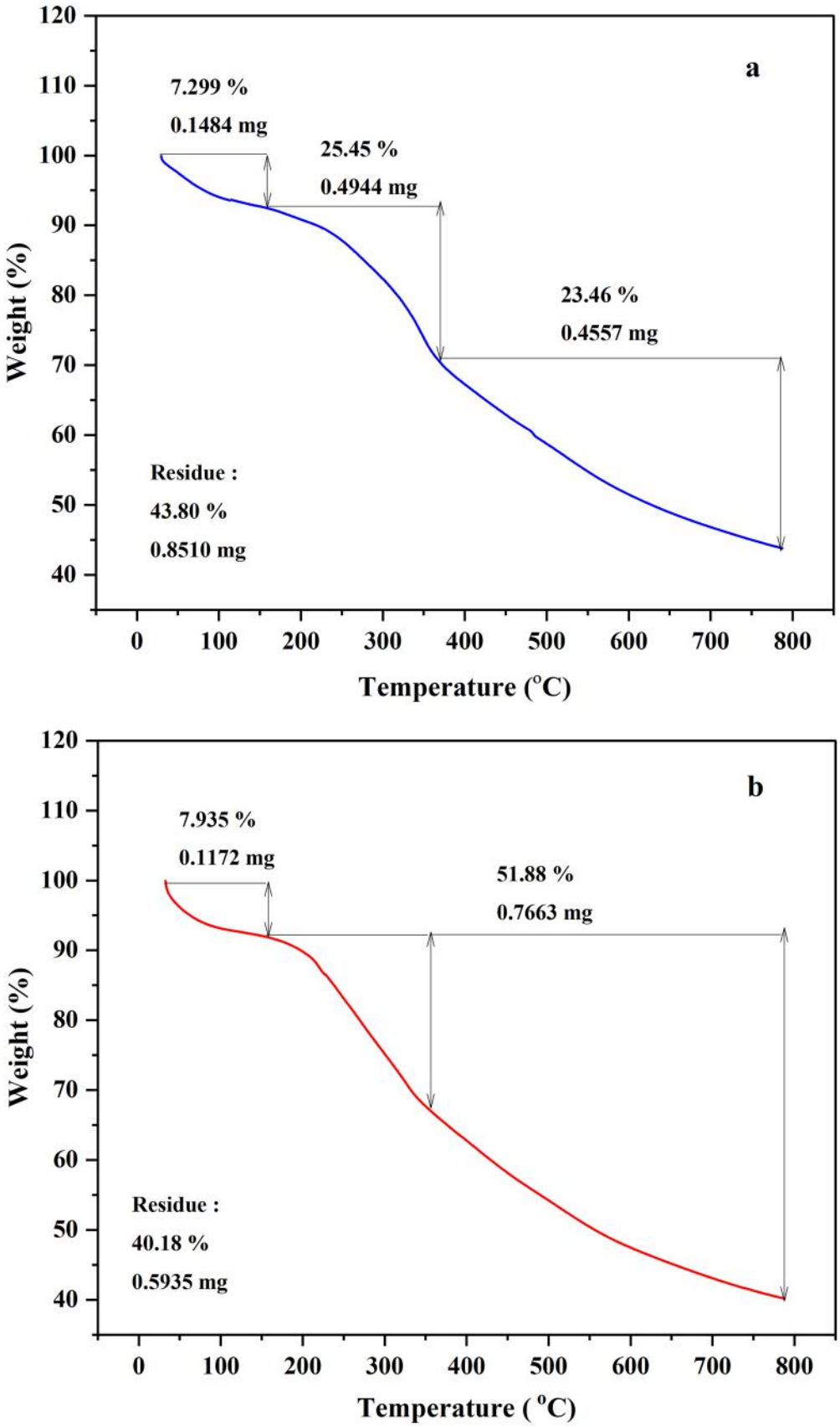

Fig. 4 TGA of (**a**) PABA (**b**) PABA-AV

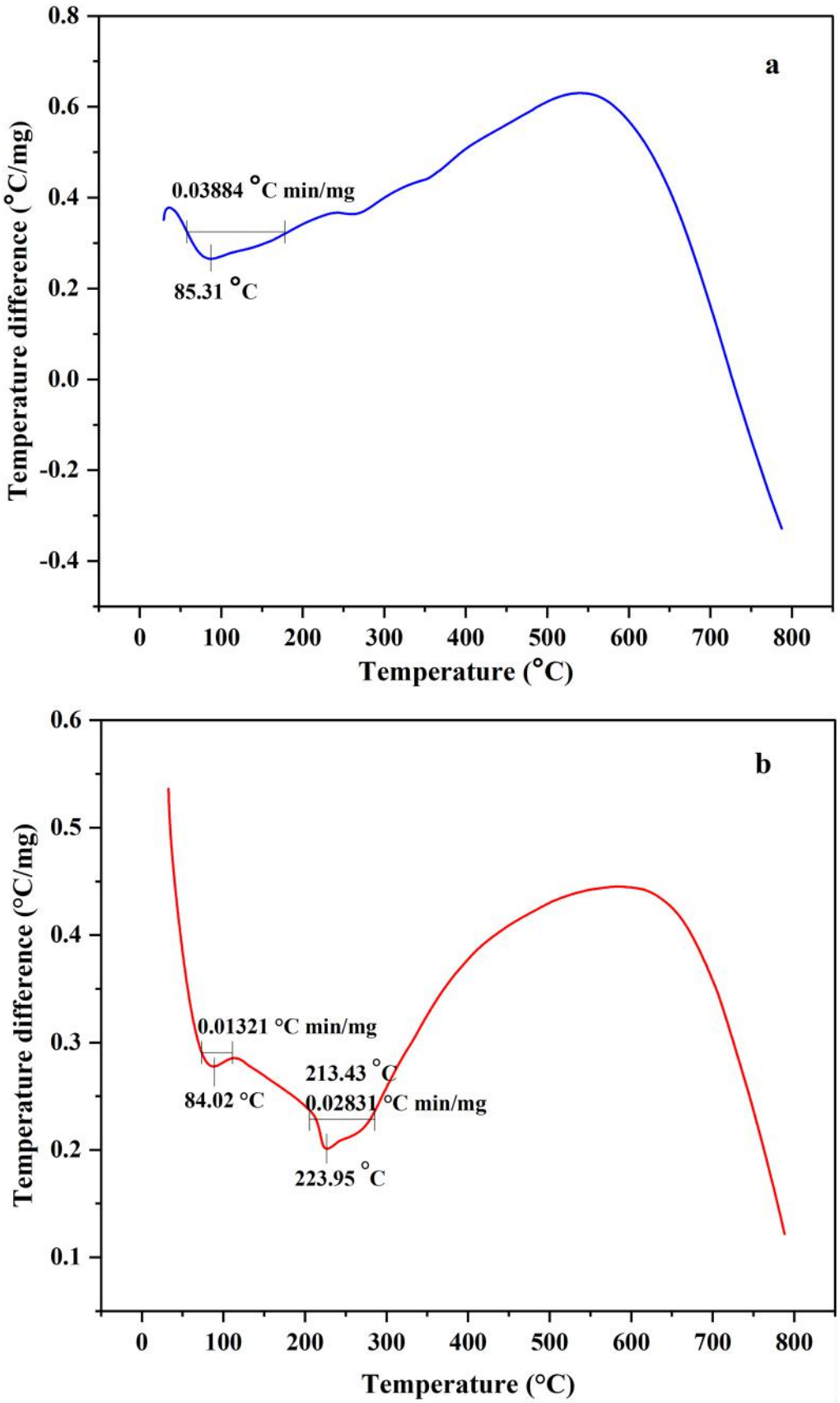

Fig. 5 DTA of (**a**) PABA (**b**) PABA-AV

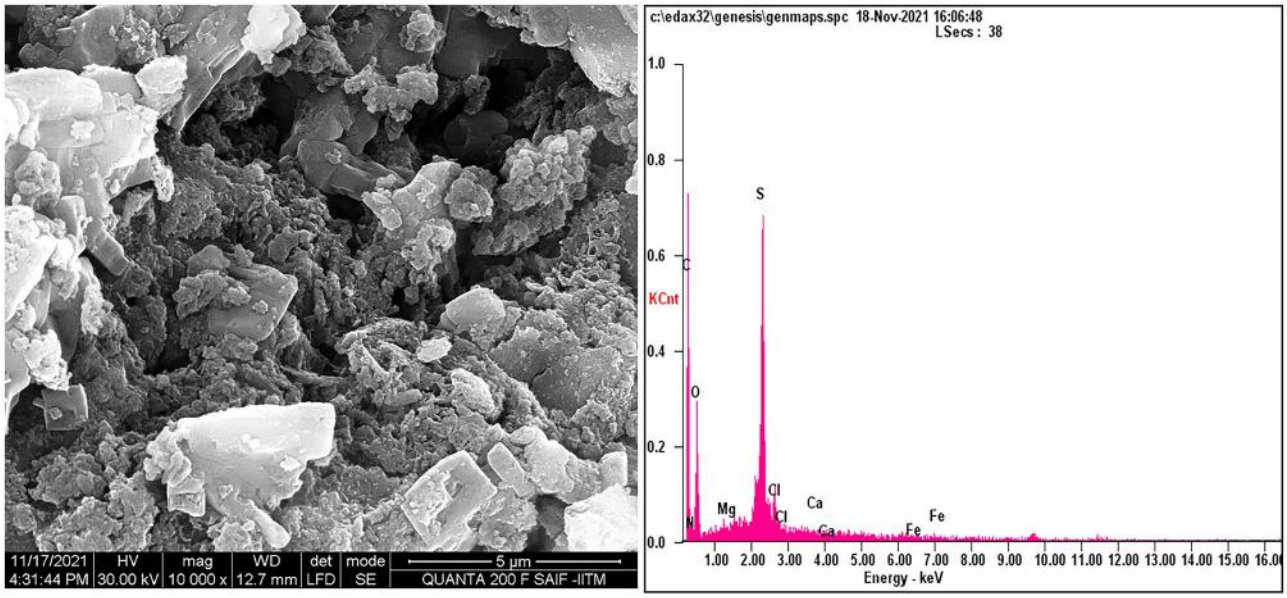

Fig. 6 SEM-EDX of PABA-AV

The Nyquist plots of PABA and PABA-AV are given in Fig.7(a) and (b) respectively. The formula, $\sigma = t/R_bA$ was used to determine the electrical conductivity where the bulk resistance 'R_b' is calculated using the Zsimpdemo software, 't' represents the thickness of the pellet and 'A' denotes the area covered by the material on the electrode [28]. The electrical conductivity values are tabulated in Table 2.

Electrochemical detection of dopamine

Electrocatalytic activity of PABA and PABA-AV

The electrocatalytic oxidation of dopamine (DA) was investigated using the bare GCE and two modified GCE with PABA and PABA-AV. It was carried out in 0.1 M PBS containing 1 mM DA at pH=7 in the potential range of -0.2 V to 0.8 V at a scan rate of 50 mV/s as shown in Fig. 8. The anodic peak corresponds to the electrochemical oxidation of dopamine to dopamine ortho-quinone and the cathodic peak corresponds to the reduction of dopamine ortho-quinone to dopamine. The anodic peak currents are seen for bare GCE, PABA/GCE and PABA-AV/GCE at I_{pa} =27.7 µA, 44.3 µA and 73.5 µA respectively. Previous studies by Huang and colleagues reported an oxidation peak current of 63.5 µA with poly(p-aminobenzoic acid)/graphene composite film-modified GCE towards the sensing of dopamine [17]. The anodic peak potential and the cathodic peak potential of PABA-AV/GCE at 0.29 V and 0.1 V respectively correspond to the oxidation and reduction of DA. Higher I_{pa} suggest PABA-AV/GCE as a suitable material for biosensing. The reason for the higher anodic current in the modified PABA-AV/GCE can be attributed to the hydrogen bonding interactions between PABA-AV and the analyte dopamine as represented in Scheme 1.

Table 1 Elemental composition of PABA-AV

S.No.	Element	At %	Wt %
1.	C	60.20	68.90
2.	N	07.30	07.16
3.	O	23.35	20.06
4.	Na	00.17	00.10
5.	Mg	00.11	00.06
6.	S	07.74	03.32
7.	Cl	00.72	00.28
8.	Ca	00.19	00.06
9.	Fe	00.24	00.06

The Laviron theory was used to find the number of electrons involved in the redox reaction of dopamine as seen in Eq. (1)

$$i_p = \frac{nFQV}{4RT} \quad (1)$$

where i_p = anodic or cathodic peak current, n = number of electrons, F = Faraday constant, Q = electric quantity, V = scan rate, R = gas constant and T = temperature

From the equation, the number of electrons was calculated and found to be 2. This implied that the modified PABA-AV/GCE facilitated 2 electrons in the oxidation of dopamine to dopamine-o-quinone and vice-versa. As equal number of protons and electrons are involved in the

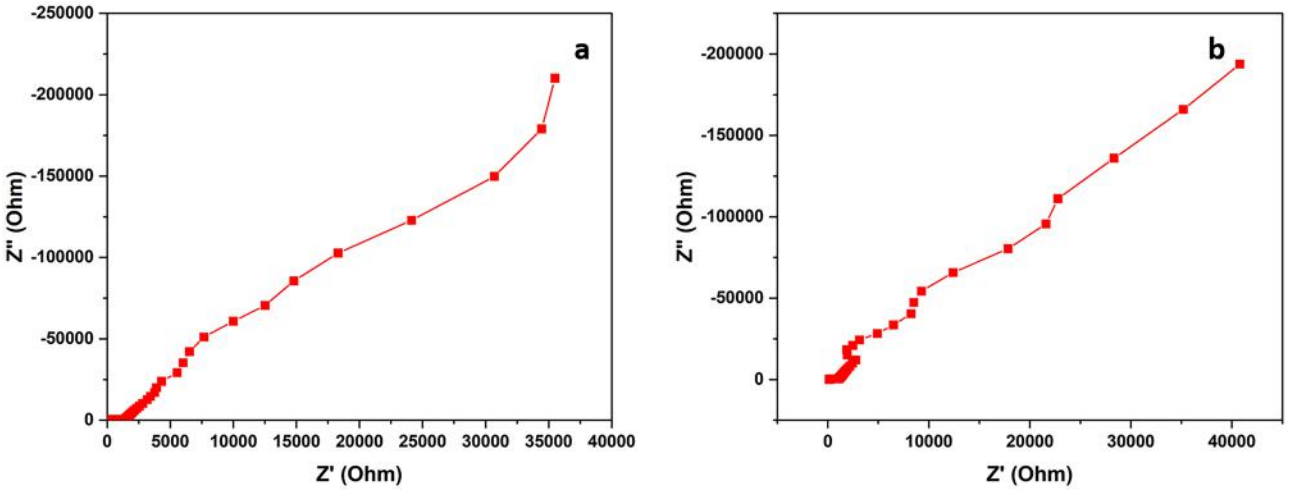

Fig. 7 Nyquist plots of (**a**) PABA (**b**) PABA-AV

electrochemical oxidation of dopamine, the number of protons involved in the reaction is also 2.

Effect of concentration

The cyclic voltammetry was carried out by using different concentrations of PABA-AV/GCE (4, 6, 8 and 10 µL) and shown in Fig. 9 by fixing the potential window from -0.2 V to 0.6 V at a scan rate of 50 mV s^{-1} in 0.1 M PBS (pH=7) with 1 mM DA. The anodic peak currents of DA increased with increase in the concentration of PABA-AV/GCE from 4 to 8 µL and decreased considerably at 10 µL. Therefore, the highest anodic peak current (I_{pa}) of 71.7 µA was observed at a concentration of 8 µL of PABA-AV/GCE and hence we fixed 8 µL as the optimum concentration for further studies.

Effect of scan rate

The scan rate was measured from 5 mVs^{-1} to 1000 mVs^{-1} in 0.1 M PBS at pH =7 with 1mM DA in the potential range of -0.2 to 0.6 V as illustrated in Fig. 10(a). As the scan rate increased, the electrochemical redox process of DA also increased. A linear plot in anodic peak currents (I_{pa}) / cathodic (I_{pc}) peak currents versus the square root of the scan rate ($\nu^{1/2}$) is depicted in Fig. 10(b). It is evident from the calibration plot that the electrochemical redox reaction of DA is a diffusion-controlled process owing to the linearity [7]. As there is an increase in the scan rate with peak potential separation (ΔE_p), the electrochemical redox reaction of DA is a quasi- reversible electrode process [29].

The linear regression analysis corresponding to the oxidation and reduction peak currents with the square root of scan rate is given in Eqs. (2 and 3) respectively.

Oxidation of DA

$$I_{pa}(mA) = 0.0008\nu^{1/2} - 0.0071(R^2 = 0.9438) \quad (2)$$

Table 2 Electrical conductivity of PABA and PABA-AV

S.No.	Polymer/ composite/ blend	Area of the electrode (A) cm^2	Thickness of the material (t) cm	Bulk Resistance (R_b) Ohm	Electrical Conductivity (σ) S cm^{-1}
1.	PABA	0.25	0.5	1363	1.5 x 10^{-3}
2.	PABA-AV	0.25	0.5	1072	1.86 x 10^{-3}

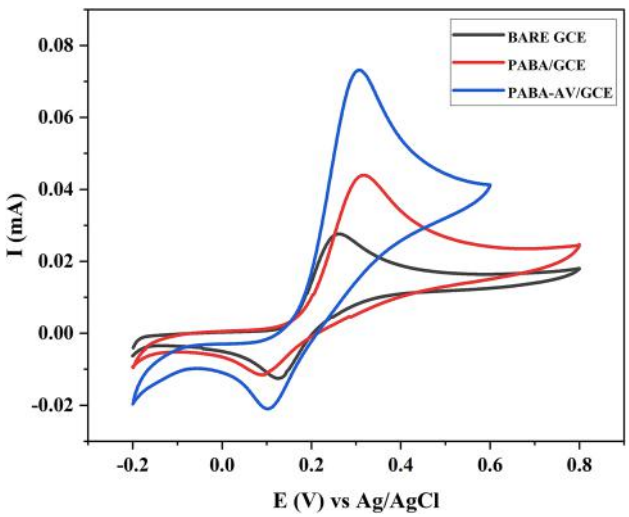

Fig. 8 Cyclic voltammograms of bare GCE, PABA/GCE and PABA-AV/GCE in 0.1M PBS at pH=7 containing 1 mM DA at 50 mVs^{-1}

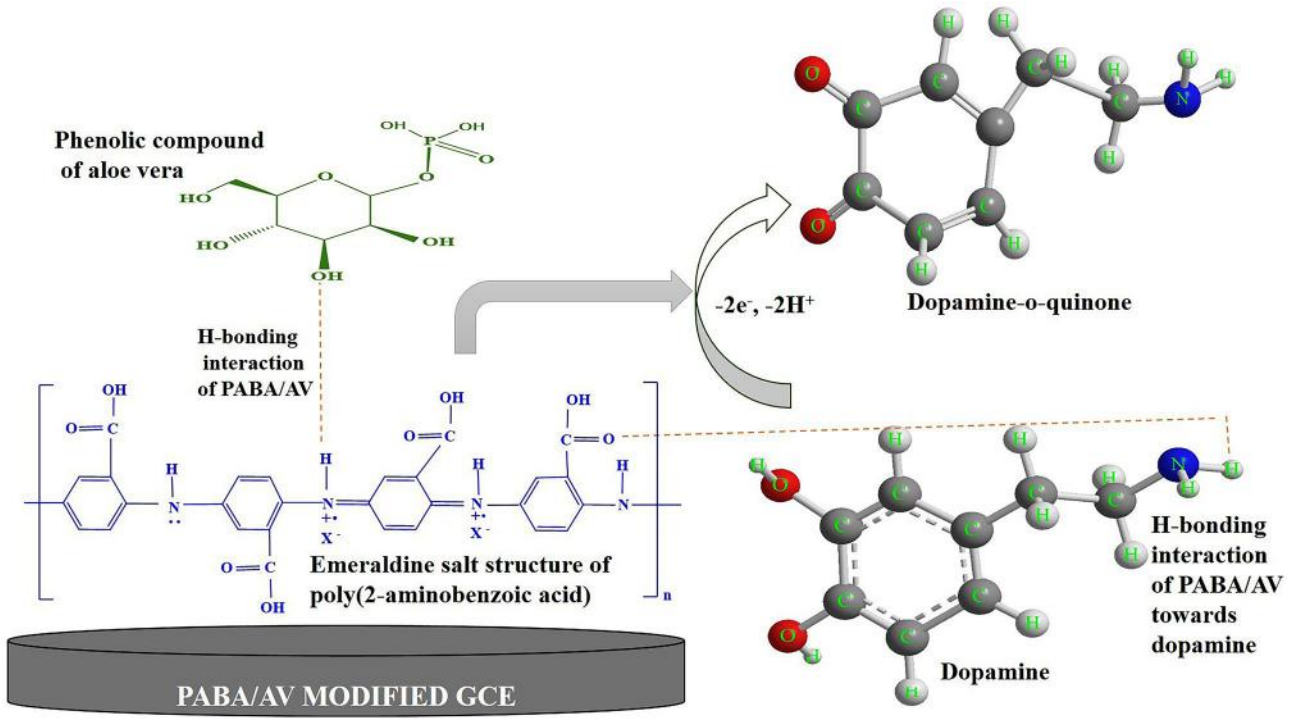

Scheme 1 Hydrogen bonding interactions of modified PABA-AV/GCE and dopamine

Reduction of DA

$$I_{pc}(mA) = 0.0009v^{1/2} - 0.0016(R^2 = 0.965) \quad (3)$$

The diffusion coefficient as calculated from Randles-Sevcik's equation is given in Eq. (4).

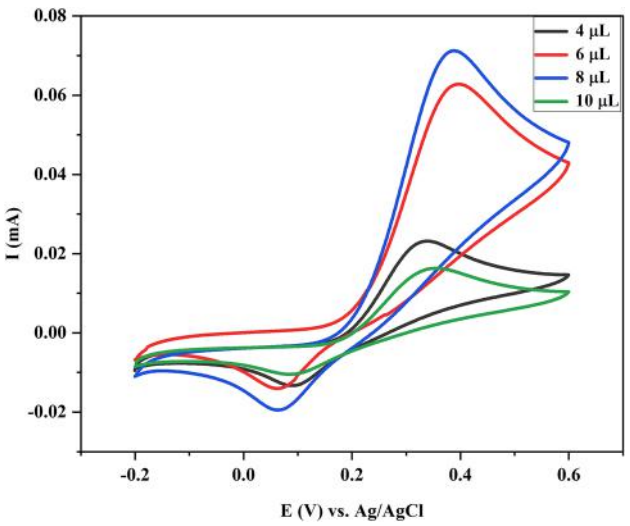

Fig. 9 Cyclic voltammograms of PABA-AV/GCE at different concentrations (4, 6, 8 and 10 µL) in 0.1 M PBS at pH=7 containing 1 mM DA at scan rate 50 mVs^{-1}

$$I_{pa} = (2.69 \times 10^{-5})n^{3/2}ACD^{1/2}v^{1/2} \quad (4)$$

where I_{pa} is the anodic peak current (µA), n is the number of electrons, A is the area of the electrode (cm^2), C is the concentration of the analyte (mM), D is the Diffusion coefficient ($cm^2\ s^{-1}$) and ν is the scan rate (Vs^{-1}). The diffusion coefficient is 17.34 x 10^{-10} $cm^2\ s^{-1}$ which also supports the diffusion-controlled mechanism.

The active surface area is calculated using Eq. (5). Q is the integrated charge of the cathodic peak at a scan rate of 50 mV/s, n is the number of electrons, A is the area of the working electrode (0.707 cm^2) and F is 96,485.3 C mol^{-1}. The active surface area is calculated as 1.013 x 10^{-4} cm^{-2} mol.

$$Electro\ active\ surface\ area = \frac{Q}{nFA} \quad (5)$$

The E_{pa} and E_{pc} versus log ν are plotted in Fig. 10(c) and it shows a linear plot for the redox reaction of DA.

The linear regression equations for the anodic (E_{pa}) and cathodic (E_{pc}) peak potential towards log ν are given below in Eqs. (6 and 7) respectively.

$$E_{pa} = 0.0591\ \log\ v + 0.1623(R^2 = 0.9580) \quad (6)$$

$$E_{pc} = -0.0372\ \log\ v + 0.1955(R^2 = 0.9623) \quad (7)$$

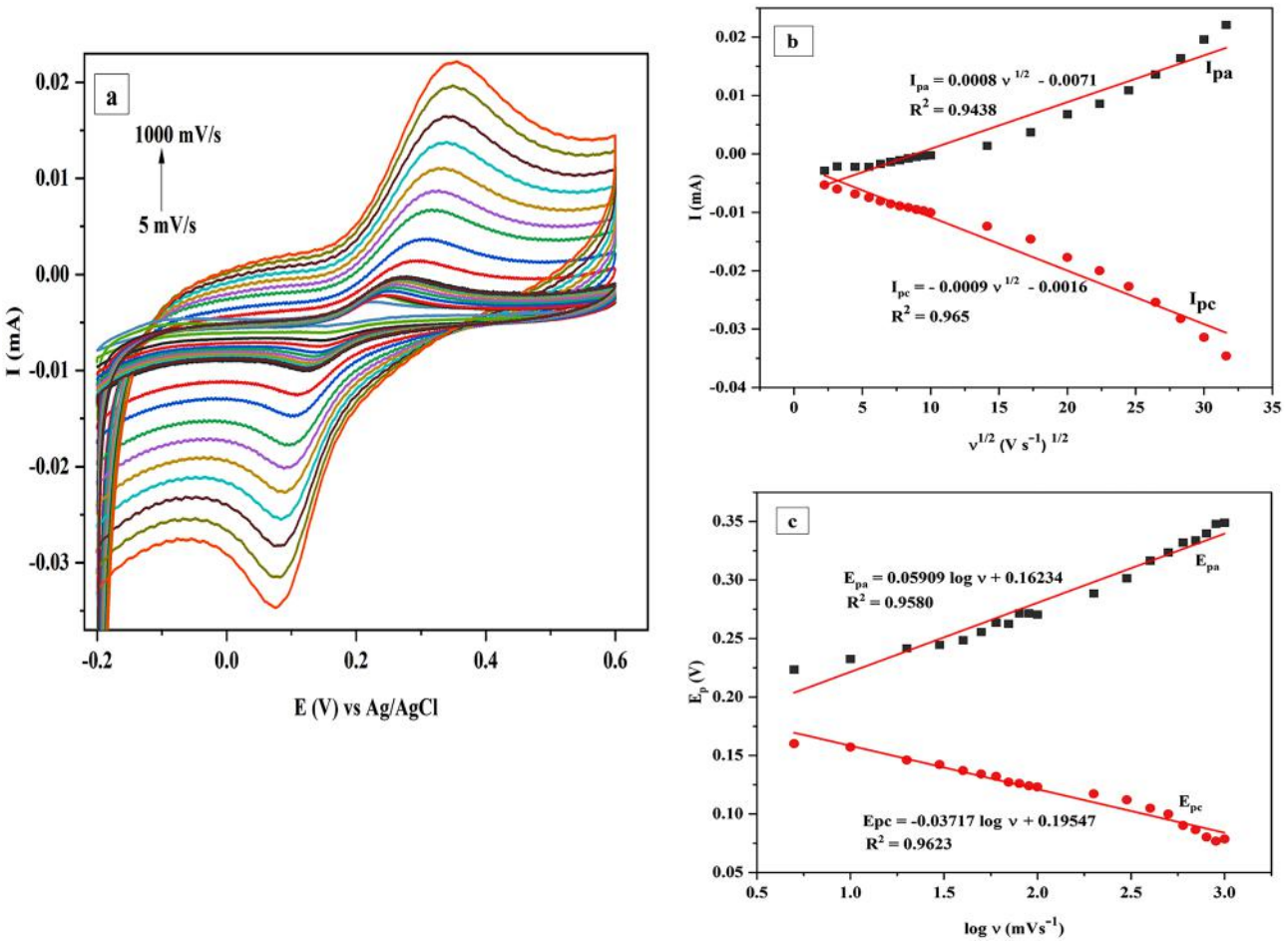

Fig. 10 Cyclic voltammograms (0.1 M PBS, pH =7, 1 mM DA) of PABA-AV/GCE at (**a**) different scan rates of 5, 10, 20, 30, 40, 50, 60, 70, 80, 90, 100, 200, 300, 400, 500, 600, 700, 800, 900 and 1000 mVs^{-1} (**b**) Linear calibration plot of I_p *vs* $\nu^{1/2}$ (**c**) Linear calibration plot of E_p *vs* log ν.

The kinetics of the electrochemical oxidation of dopamine using modified PABA-AV/GCE is determined by the electron transfer coefficient (α) and the heterogeneous electron transfer rate constant (k_s) given in Eqs. (8 and 9) respectively. k_a and k_c are the slopes obtained by linear regression analysis of anodic peak current and cathodic peak current respectively (Eqs. 6 and 7). The electron transfer coefficient α calculated is 0.61 and the electron transfer rate constant is 0.0243 s^{-1}. An efficient electron transfer reaction is facilitated between the modified PABA-AV/GCE and dopamine.

$$\frac{ka}{kc} = -\frac{\alpha}{(1-\alpha)} \tag{8}$$

$$\log\ k_s = \alpha\ \log\ (1-\alpha) + (1-\alpha)\ log\ \alpha - log\frac{RT}{nFv} - \frac{\alpha(1-\alpha)nF\Delta EP}{2.303RT} \tag{9}$$

Effect of pH

Proton transfer at the electrode-solution interface is greatly influenced by the composition and pH of the supporting electrolytes. Hence, the effect of pH on the electrochemical redox reaction was studied at 50 mV/s in 0.1 M PBS at different pH of 3, 5, 7, 9 and 11 as shown in Fig. 11. The pH was adjusted by the addition of H_3PO_3 to make it acidic and NaOH to make it basic. The highest anodic current generated is 73.5 µA at pH =7. Lesser peak currents were observed in basic pH and no oxidation peaks in the acidic pH range. The anodic peak potentials shifted to lower potentials at high pH and hence we selected pH 7 for further study.

Differential pulse voltammetry

The DPV parameters were setup as pulse height P_H = 25 mV, pulse width P_W = 50 ms, step height S_H = 50 mV and

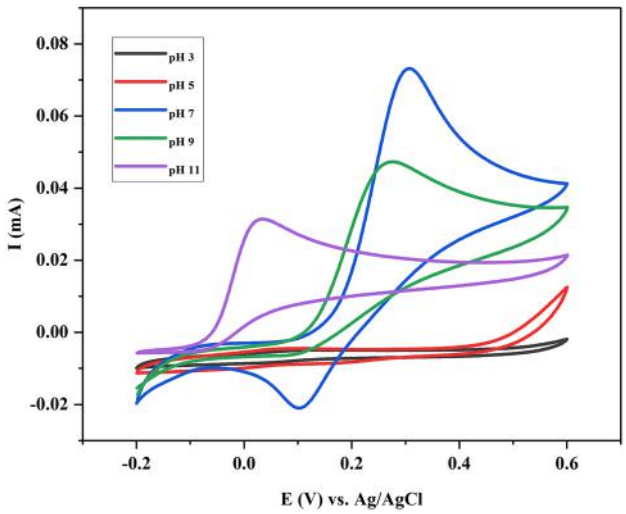

Fig. 11 Cyclic voltammograms of PABA-AV/GCE in 0.1M PBS containing 1mm DA at different pH of 3, 5, 7, 9 and 11 at a scan rate of 50 mVs^{-1}

step time S_T= 100 ms. The concentration of dopamine was increased from 100 - 800 µM and their significance on the anodic current response was recorded and represented in Fig. 12. The anodic oxidation peak currents of DA increased with an increase in the concentration of dopamine. The calibration plot depicted a linear relation between DA concentration and anodic current [$I_{pa}(\mu A) = 52.6428 + 0.0252\ C_{DA}(\mu M)$ ($R^2 = 0.9982$)] in the concentration range of 100 - 800 µM.

The limit of detection (LOD) and limit of quantification (LOQ) of DA at pH=7 is 0.0517 µM and 0.1722 µM respectively in the linear dynamic range of 100-800 µM. The sensitivity is 0.0357 $\mu A \mu M^{-1} cm^{-2}$ in the linear range 100-800 µM. The current response upon increasing concentrations of DA is mainly due to two reasons i.e. electrostatic interaction and hydrogen bonding. The electrostatic attraction is prevalent in polymer systems owing to the amino groups and carboxyl groups present in dopamine and PABA-AV. The functional groups such as carboxyl, hydroxyl and amine groups present in abundance in PABA-AV/GCE interact with the amine group of the analyte dopamine through hydrogen bonding and π- π stacking interactions between the phenyl structure of DA and the benzenoid structure of PABA-AV/GCE [30, 31].

We would like to point out that the fabricated sensor of the synthesized polymer blend has a lower limit of detection as compared to other polyaniline-based nanocomposites/blends previously reported in the literature. The results have been enlisted in Table 3 given below.

Table 3 Comparison of the proposed PABA-AV electrode to other modified electrodes for the determination of dopamine

S. No.	Modified electrode	Linear range (µmol/L)	Detection limit (µmol/L)	Reference
1.	rGO-PpPD/GCE	50-200	0.36	[32]
2.	POMA-Au/GCE	10-300	0.062	[16]
3.	POA/CNTs/GCE	10-260	0.12	[33]
4.	V_2O_5@PANI	6.6-110	39	[34]
5.	PANI/CQDs	10-90	0.1013	[30]
6.	GNPs/PANI	3-115	0.8	[15]
7.	PANI/MWCNTs	50-385	38	[35]
8.	AuNPs@PANI	10-1700	5	[31]
9.	AuNPs/MoS_2-PANI/GCE	1-500	0.1	[36]
10.	**PABA-AV/GCE**	**100-800**	**0.0517**	**This work**

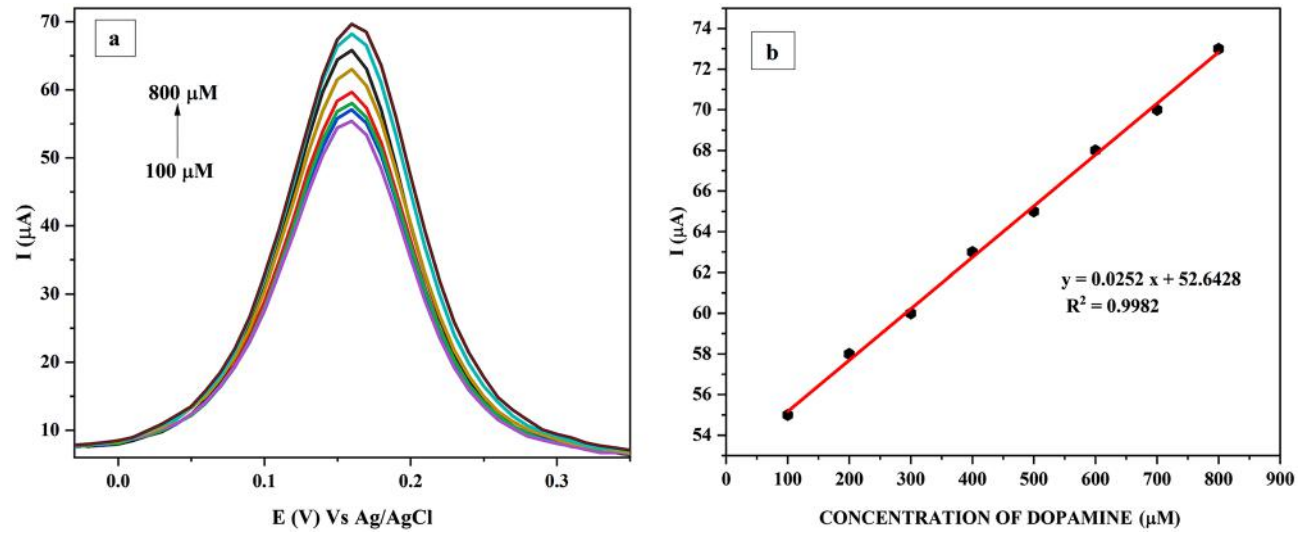

Fig. 12 (**a**) Differential pulse voltammograms of PABA-AV/GCE in the dopamine concentration range of 100 to 800 µM (**b**) Calibration plot

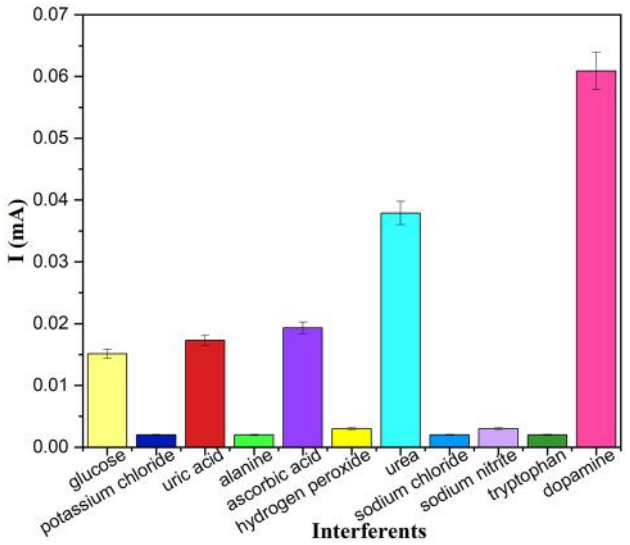

Fig. 13 Selectivity of PABA-AV/GCE modified electrode against various interferents

Effect of interferents

The interference analysis was performed by cyclic voltammetry with a wide range of interferents at 50 mV/s as shown in Fig. 13. The interferents selected for the study were glucose, potassium chloride, uric acid, alanine, ascorbic acid, hydrogen peroxide, urea, sodium chloride, sodium nitrite and tryptophan. 50 µL of 1M interferent was added into the PBS solution followed by the addition of 100 µL of dopamine. Even in the presence of a wide range of interferences, PABA-AV/GCE could sense dopamine at 0.29 V with a current of 0.06 mA proving the highly selective nature of the electrocatalyst.

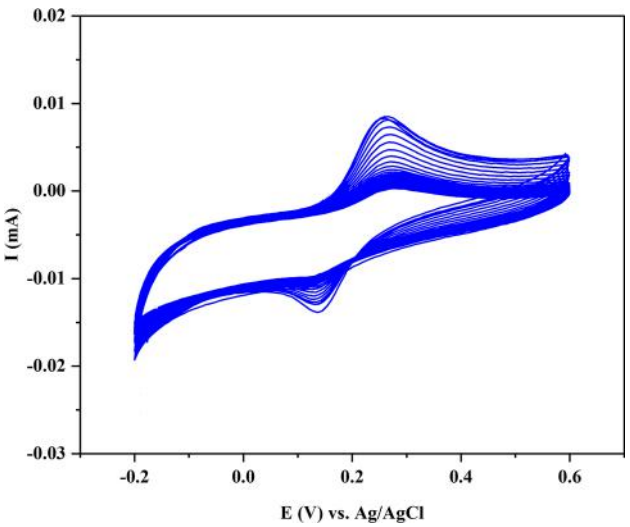

Fig. 14 Repeatability of PABA-AV/GCE at 50 successive CV cycles

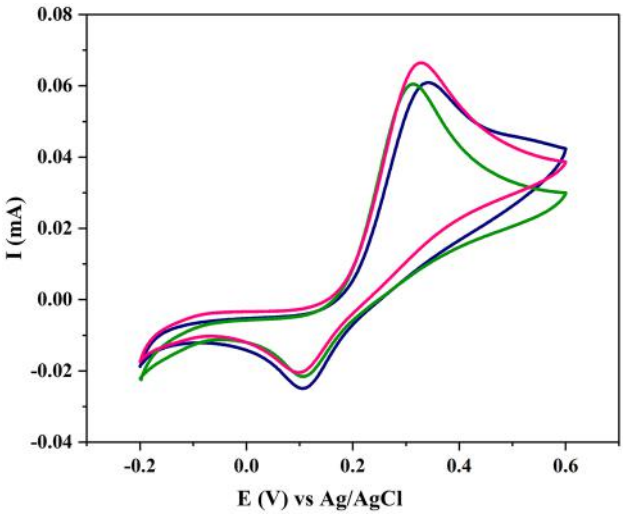

Fig. 15 Reproducibility of PABA-AV/GCE

Repeatability, reproducibility and stability

PABA-AV/GCE demonstrates appreciable repeatability at 50 successive CV cycles in 0.1 M PBS (pH=7) containing 1 mM DA as shown in Fig. 14. The reproducibility of the modified PABA-AV/GCE was carried out independently 3 times with the same experimental setup (0.1 M PBS, pH=7, 1 mM DA) using cyclic voltammetry as given in Fig. 15. The modified electrode exhibited an R.S.D. of 5.3% and showed considerable reproducibility. The stability of the modified electrode was calculated by storing the electrode in the refrigerator at 4° C for 2 weeks. On day 1, the fabricated electrode exhibited a current response of 73.7 µA and on day 14, the current response against dopamine was recorded to be 69.7 µA. It was noted that the modified PABA-AV/GCE lost only 5.427 % of dopamine response even after 2 weeks displaying its outstanding stability. Thus, the fabricated PABA-AV/GCE modified electrode proves efficient with acceptable repeatability, reproducibility and stability.

Conclusion

In summary, PABA and PABA-AV were synthesized by the emulsion polymerization method and characterized by FT-IR, UV-Visible, XRD, TGA/DTA, SEM-EDX and EIS. The high conducting capability, redox activity and biocompatibility of the polymer and its blend proved them to be efficient candidates for detecting the neurotransmitter dopamine. PABA-AV/GCE modified electrode contributed efficiently to the electrocatalytic oxidation of dopamine in the wide linear concentration range of 100-800 µM with a limit of detection of 0.0517 µM (S/N=3) and a limit of

quantification of 0.1722 μM (S/N=10) respectively. The sensitivity of the fabricated electrochemical biosensor was 0.0357 $\mu A \mu M^{-1} cm^{-2}$ in this linear range. The modified electrode exhibited high selectivity towards dopamine even in the presence of interferents such as alanine, glucose, hydrogen peroxide, potassium chloride, sodium chloride, sodium nitrite, tryptophan, uric acid, urea and ascorbic acid. PABA-AV/GCE modified electrode shows appreciable selectivity, repeatability, reproducibility and stability making it a promising material in the field of biosensors.

Data availability The data supporting this study can be made available upon request.

Declarations

Conflicts of interest The author(s) declare that there is no conflict of interest with respect to the research, authorship and/or publication of this article.

References

1. Liu S, Xing XR, Yu JH, Lian W, Li J, Cui M, Huang J (2012) A novel label-free electrochemical aptasensor based on graphene-polyaniline composite film for dopamine determination. Biosens Bioelectron 36:186–191
2. Zhang Y, Yuan R, Chai Y, Li W, Zhong X, Zhong H (2011) Simultaneous voltammetric determination for DA, AA and NO_2 based on graphene/poly-cyclodextrin/MWCNTs nanocomposite platform. Biosens Bioelectron 26:3977–3980
3. Zhao Y, Zhao S, Huang J, Ye F (2011) Quantum dot-enhanced chemiluminescence detection for simultaneous determination of dopamine and epinephrine by capillary electrophoresis. Talanta 85:2650–2654
4. Huang HM, Lin CH (2005) Methanol plug assisted sweeping-micellar electrokinetic chromatography for the determination of dopamine in urine by violet light emitting diode-induced fluorescence detection. J Chromatogr B 816:113–119
5. Li L, Liu H, Shen Y, Zhang J, Zhu JJ (2011) Electrogenerated chemiluminescence of au nanoclusters for the detection of dopamine. Anal Chem 83:661–665
6. Carrera V, Sabater E, Vilanova E, Sogorb MA (2007) A simple and rapid HPLC-MS method for the simultaneous determination of epinephrine, norepinephrine, dopamine and 5-hydroxytryptamine: application to the secretion of bovine chromaffin cell cultures. J Chromatogr B 847:88–94
7. Xie LQ, Zhang YH, Gao F, Wu QA, Xu PY, Wang SS, Gao NN, Wang QX (2017) A highly sensitive dopamine sensor based on a polyaniline/reduced graphene oxide/Nafion nanocomposite. Chin Chem Lett 28:41–48
8. Arumugasamy SK, Govindaraju S, Yun K (2020) Electrochemical sensor for detecting dopamine using graphene quantum dots incorporated with multiwall carbon nanotubes. Appl Surf Sci 508:145294
9. Zhu Z, Qu L, Guo Y, Zeng Y, Sun W, Huang X (2010) Electrochemical detection of dopamine on a Ni/Al layered double hydroxide modified carbon ionic liquid electrode. Sens Actuators B Chem 151:146–152
10. Yusoff N, Pandikumar A, Ramaraj R, Lim HN, Huang NM (2015) Gold nanoparticle based optical and electrochemical sensing of dopamine. Microchim Acta 182:2091–2114
11. Wang W, Xu G, Cui XT, Sheng G, Luo X (2014) Enhanced catalytic and dopamine sensing properties of electrochemically reduced conducting polymer nanocomposite doped with pure graphene oxide. Biosens Bioelectron 58:153–156
12. Tavakol S, Hoveizi E, Tavakol H, Almasi A, Soleimani M, Rabiee M, Shadi A, Fereshteh J, Mohammad T (2022) Strong binding of phytochemicals to the catalytic domain of tyrosine hydroxylase as a trojan horse decreases dopamine in dopaminergic cells: Pharmaceutical considerations in Schizophrenia and Parkinson's disease 28:3428–3445
13. Sundar S, Venkatachalam G, Kwon SJ (2018) Sol-gel mediated greener synthesis of ɣ-Fe_2O_3 nanostructures for the selective and sensitive determination of uric acid and dopamine. Catalysts 8:512
14. Fayemi OE, Adekunle AS, Kumara Swamy BE, Ebenso EE (2018) Electrochemical sensor for the detection of dopamine in real samples using polyaniline/NiO, ZnO, and Fe_3O_4 nanocomposites on glassy carbon electrode. J Electroanal Chem 818:236–249
15. Wang AJ, Feng JJ, Li YF, Xi JL, Dong WJ (2010) In-situ decorated gold nanoparticles on polyaniline with enhanced electrocatalysis toward dopamine. Microchim Acta 171:431–436
16. Sangamithirai D, Munusamy S, Narayanan V, Stephen A (2018) A voltammetric biosensor based on poly(o-methoxyaniline)-gold nanocomposite modified electrode for the simultaneous determination of dopamine and folic acid. Mater Sci Eng C 91:512–523
17. Huang KJ, Jing QS, Wu ZW, Wang L, Wei CY (2011) Enhanced sensing of dopamine in the presence of ascorbic acid based on graphene/poly(p-aminobenzoic acid) composite film. Colloids Surf B: Biointerfaces 88:310–314
18. Gupta B, Melvin A, Prakash R (2014) Synthesis of polyanthranilic acid-Au nanocomposites by emulsion polymerization: development of dopamine sensor. Bull Mater Sci 37:1389–1395
19. Taleat Z, Ravalli A, Ardakani MM, Marrazza G (2012) CA 125 immunosensor based on poly-anthranilic acid modified screen-printed electrodes. Electroanalysis 25:269–277
20. Bilal S, Gul S, Holze R, Ali Shah AH (2015) An impressive emulsion polymerization route for the synthesis of highly soluble and conducting polyaniline salts. Synth Met 206:131–144
21. Barandozi FM, Enferadi ST (2012) FT-IR study of the polysaccharides isolated from the skin juice, gel juice, and flower of aloe vera tissues affected by fertilizer treatment. Org Med Chem Lett 2:1–9
22. Tang J, Jing X, Wang B, Wang F (1988) Infrared spectra of soluble polyaniline. Synth Met 24:231–238
23. Gupta DK, Neupane S, Singh S, Karki N, Yadav AP (2021) The effect of electrolytes on the coating of polyaniline on mild steel by electrochemical methods and its corrosion behaviour. Prog Org Coat 152:106127
24. Zoromba MS, Alshehri AA, Al-hossainy AF, Abdel-aziz MH (2021) Doped-poly(anthranilic acid-co-o-phenylene diamine) thin film for optoelectronic applications. Opt Mater 111:110621
25. Wang S, Tan Z, Li Y, Sun L, Zhang T (2006) Synthesis, characterization and thermal analysis of polyaniline/ZrO_2 composites. Thermochim Acta 441:191–194
26. Jayakrishnan P, Ramesan MT (2017) Synthesis, structural, magnetoelectric and thermal properties of poly(anthranilic acid)/magnetite nanocomposites. Polym Bull 74:3179–3198
27. Zoromba MS, Belal AAM, Al-Hussaini AS (2015) From copolymer precursor to metal oxides nanoparticles: synthesis and characterization of doped copper and cobalt copolymer via in situ and ex situ copolymerization. J Macromol Sci Part A Pure Appl Chem 52:394–400
28. Jayakrishnan P, Ramesan MT (2017) Temperature dependence of the electrical conductivity of poly(anthranilic acid)/magnetite nanocomposites and the applicability of different conductivity models. Polym Compos 39:2791–2800
29. Mathew G, Dey P, Das R, Chowdhury SD, Das MP, Veluswamy P, Neppolian B, Das J (2018) Direct electrochemical reduction of hematite decorated graphene oxide (α-Fe_2O_3@erGO)

nanocomposite for selective detection of Parkinson's disease biomarker. Biosens Bioelectron 115:53–60
30. Ratlam C, Phanichphant S, Sriwichai S (2020) Development of dopamine biosensor based on polyaniline/carbon quantum dots composite. J Polym Res 27:183
31. Yang L, Liu S, Zhang Q, Li F (2012) Simultaneous electrochemical determination of dopamine and ascorbic acid using AuNPs@polyaniline core- shell nanocomposites modified electrode. Talanta 89:136–141
32. Liu S, Yu B, Zhang T (2013) Preparation of crumpled reduced graphene oxide-poly(p- phenylenediamine) hybrids for the detection of dopamine. J Mater Chem A 1:13314–13320
33. Sangamithirai D, Munusamy S, Narayanan V, Stephen A (2016) Fabrication of neurotransmitter dopamine electrochemical sensor based on poly(o-anisidine)/CNTs nanocomposite. Surf Interfaces 4:27–34
34. Suresh R, Giribabu K, Manigandan R, Praveen Kumar S, Munusamy S, Muthamizh S, Narayanan V (2014) Characterization and dopamine sensing property of V_2O_5@polyailinenanohybrid. Synth Met 196:151–157
35. Sabzi RE, Rezapour K, Samadi N (2010) Polyaniline-multi-wall-carbon nanotube nanocomposites as a dopamine sensor. J Serb Chem Soc 75:537–549
36. Huang KJ, Zhang JZ, Liu YJ, Wang LL (2014) Novel electrochemical sensing platform based on molybdenum disulfide nanosheets- polyaniline composites and au nanoparticles. Sens Actuators B Chem 194:303–310